Int J Adv Manuf Technol (2009) 43:862–871
DOI 10.1007/s00170-008-1764-2

ORIGINAL ARTICLE

Stability analysis of turning process with tailstock-supported workpiece

M. Sekar · J. Srinivas · K. Rama Kotaiah · S. H. Yang

Received: 22 March 2008 / Accepted: 15 September 2008 / Published online: 15 October 2008

Abstract This paper proposes an analytical scheme for stability analysis in turning process by considering the motion of tailstock-supported workpiece using a compliance model of tool and work. A dynamic cutting force model based on relative motion between the cutting tool and workpiece is developed to study the chatter stability. Linear stability analysis is carried out in the frequency domain and the stability charts are obtained with and without considering workpiece flexibility. Variations of stability limits with workpiece dimensions and cutter position as well as the effects of cutting tool dynamics are studied and wherever possible results are compared with existing models. Experimental analysis is conducted on tailstock-supported workpiece to examine the correctness of the proposed stability model.

Keywords Chatter stability · Regeneration · Compliance · Two-degree model · Critical parameters

1 Introduction

To achieve high material removal rates in production, aggressive cutting conditions are often used. Such conditions lead to chatter where intensive and excessive cutting forces occur at the cutting point. In order to obtain chatter-free machining conditions, conservative cutting conditions are often used which result in lower material removal rates and loss of productivity. Therefore, the stability limit should be predicted to enhance material removal rate while maintaining product quality.

Analytical prediction of stability limits for orthogonal cutting is well documented in literature [1–5]. Basically, the turning tool is represented with a single degree for freedom spring-mass system working over a rigid workpiece. Cutting tool parameters such as tool angles and wear have been accounted in the models to understand their effects on chatter stability. In general, regenerative and nonregenerative chatters are two kinds of machine tool chatter that are widely accepted in modern research. Regenerative chatter results from cutting on the previous surface of waves and nonregenerative chatter occurs due to some special circumstances. In most cases, the chatter observed in turning operations is due to regenerative effect. One of the early regenerative chatter analysis method deals with the development of a characteristic equation to determine system stability through Nyquist criterion. In practice, chatter is a self-excited oscillatory phenomenon with a highly nonlinear nature characterized by the presence of limit cycles and subcritical bifurcations related to jump phenomenon. Different models are presented in the literature for development of analytical techniques for stability analysis. Chandiramani and Pothala [6] depicted dynamics of chatter with two degrees of freedom model of cutting tool. Since chatter is due to interaction between tool and work, often the models in terms of both tool and work are considered. Dassanayake and Suh [7] studied the tool chatter with turning dynamics using a 3D model. Here, the workpiece is modeled as a system of three rotors namely machined, being machined, and unmachined

K. R. Kotaiah
K.L. College of Engineering,
Vaddeswaram,
Vijayawada, India

M. Sekar · J. Srinivas (✉) · S. H. Yang
School of Mechanical Engineering,
Kyungpook National University,
Daegu, South Korea
e-mail: srin07@yahoo.co.in

regions connected by flexible shaft. Wang and Cleghorn [8] developed a finite-element beam model of spinning stepped-shaft workpiece to perform stability analysis using Nyquist criterion. Ganguli et al. [9] showed the effect of active damping on regenerative chatter instability in turning. Tarng et al. [10] presented a spindle speed regulation method to avoid regenerative chatter in turning. Carrino et al. [11] pointed out the dimensional deviations occurring during machining of a part due to workpiece deflections, vibrations of tool, material spring back, etc. Wang and Fei [12] proposed a method based on variable stiffness in boring bars to suppress chatter. This is based on the principle of avoidance of self-excited vibrations by continuously varying the natural frequency of a structure over a range. Chen and Tsao presented a dynamic model of cutting tool with [13] and without [14] tailstock-supported workpiece using beam theory. Here, the effects of workpiece parameters are studied on the dynamic stability of turning process by treating the workpiece as a continuous system. To the author's knowledge, there are few works which considered the effects of deflections of tailstock-supported workpieces.

The present paper proposes a compliant two degrees of freedom dynamic cutting force model by considering the relative motion of workpiece with cutting tool. Tool and workpiece are modeled as two separate single degree of freedom spring-mass-damper systems. The model allows selection of different operating conditions with and without a tailstock support by accounting the fundamental natural frequency of the workpiece. Overall transfer matrix is derived from the equations of motion in the Laplacian domain and the expressions for critical parameters of cutting process in stable conditions are obtained analytically. Effect of workpiece parameters such as linear and lateral dimensions and cutter positions as well as influence of flexibility and damping of cutter on the stability is studied. In verifying the proposed model, experimental analysis is conducted on an engine lathe with a tailstock-supported steel workpiece under various operating conditions. Dynamic cutting forces are recorded with a tool dynamometer and the modal data for the workpiece and tool are obtained with standard impact hammer testing. Experimental test points are superimposed on the analytical lobe diagram in predicting the correctness of stable states.

2 Dynamic modeling

2.1 Rigid workpiece

In most of the turning operations, workpiece is considered as a rigid member and the chip thickness is assumed to be affected only by the dynamic parameters of cutting tool. This one-dimensional second-order orthogonal cutting model shown in Fig. 1 is represented with the governing equation as follows:

$$m_1\ddot{x}(t) + c_1\dot{x}(t) + k_1x(t) = F(t)\cos\theta \tag{1}$$

Here, $x(t)$ is chip thickness (variation in depth of cut) at a time t and the parameters m_1, c_1, and k_1 are the equivalent mass, damping, and stiffness of the cutting tool and tool holder, θ is a constant cutting angle and $F(t)$ is cutting force, which is given by:

$$F(t) = Cbh(t) \tag{2}$$

where C is cutting coefficient obtained from experiments and b is depth of cut or chip width. The instantaneous chip thickness $h(t)$ can be written from Fig. 1 as:

$$h(t) = h_0 - x(t) + x(t-\tau) \tag{3}$$

Here, $x(t-\tau)$ is chip thickness in previous instant; h_0 is nominal chip thickness resulting from feed mechanism and the term $x(t)-x(t-\tau)$ represents the regenerative chatter. Time delay τ represents the period for successive passages of tool, which is equal to time required for one revolution of workpiece in turning.

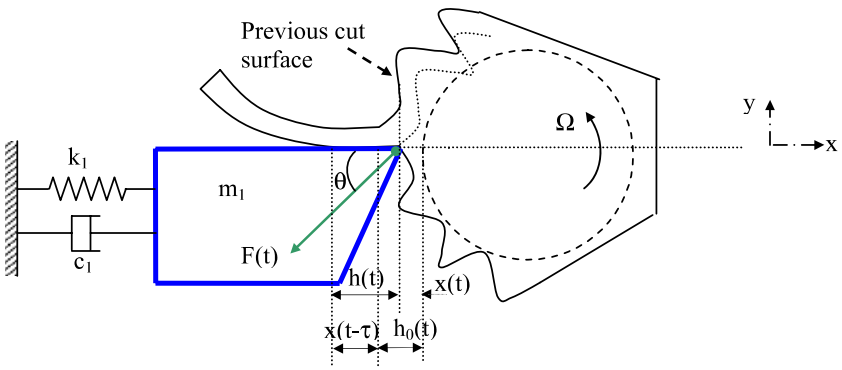

Fig. 1 Cutting tool model with rigid workpiece

Substituting Eqs. 2 and 3 in Eq. 1 and taking Laplace transforms on both sides, the dynamic equation in Laplacian (s) domain becomes:

$$\left(m_1 s^2 + c_1 s + k_1\right) X(s) = C\, b\left(H_0(s) - X(s) + e^{-s\tau} X(s)\right) \tag{4}$$

Thus, overall transfer function becomes

$$\frac{X(s)}{H_0(s)} = \frac{bCG(s)}{1 + bCG(s)(1 - e^{-s\tau})} \tag{5}$$

where

$$G(s) = \frac{\cos\theta}{m_1 s^2 + c_1 s + k_1} \tag{6}$$

2.2 Flexible workpiece

Usually, the operating spindle speeds are well below the natural frequency of workpiece. Hence, in the flexibility considerations, the first mode of vibration is considered as significant and the workpiece is represented as another single degree of freedom spring-mass-damper system as shown in Fig. 2. Here m_2, c_2, and k_2 respectively represent mass, damping coefficient, and stiffness of the workpiece. For this combined system, the equations of motion can be written in terms of tool and workpiece deformations $x_1(t)$ and $x_2(t)$ at a time t as follows:

$$m_1 \ddot{x}_1(t) + c_1 \dot{x}_1(t) + k_1 x_1(t) = -F(t)\cos\theta \tag{7}$$

$$m_2 \ddot{x}_2(t) + c_2 \dot{x}_2(t) + k_2 x_2(t) = F(t)\cos\theta \tag{8}$$

Here, $F(t)$ is dynamic feed force expressed in terms of the present and previous relative motions $(x_1(t) - x_2(t))$ and $(x_1(t-\tau) - x_2(t-\tau))$ according to:

$$F(t) = Cb\{h_0 - (x_1(t) - x_2(t)) + (x_1(t-\tau) - x_2(t-\tau))\} \tag{9}$$

When the above force term $F(t)$ in Eq. 9 is substituted in Eqs. 7 and 8 and writing $k_1/m_1 = \omega_{n1}^2$, $k_2/m_2 = \omega_{n2}^2$, $c_1/m_1 = 2\xi_1\omega_{n1}$, and $c_2/m_2 = 2\xi_2\omega_{n2}$, these two equations become coupled dynamic equations in terms of the variables x_1 and x_2 as follows:

$$\ddot{x}_1(t) + 2\xi_1\omega_{n1}\dot{x}_1(t) + \omega_{n1}^2 x_1(t) = -\frac{Cb\cos\theta}{m_1}\{h_0 - (x_1(t) - x_2(t)) + (x_1(t-\tau) - x_2(t-\tau))\} \tag{10}$$

$$\ddot{x}_2(t) + 2\xi_2\omega_{n2}\dot{x}_2(t) + \omega_{n2}^2 x_2(t) = \frac{Cb\cos\theta}{m_2}\{h_0 - (x_1(t) - x_2(t)) + (x_1(t-\tau) - x_2(t-\tau))\} \tag{11}$$

Here, ω_{n1}, ω_{n2} and ξ_1, ξ_2 are natural frequencies and damping ratios of the cutter and workpiece, respectively.

In Laplacian domain, Eqs. 10 and 11 can be written as:

$$s^2 X_1(s) + 2\xi_1\omega_{n1} s X_1(s) + \omega_{n1}^2 X_1(s) = -\frac{Cb\cos\theta}{m_1}\{H_0(s) - (1 - e^{-\tau s})X_1(s) + (1 - e^{-\tau s})X_2(s)\} \tag{12}$$

$$s^2 X_2(s) + 2\xi_2\omega_{n2} s X_2(s) + \omega_{n2}^2 X_2(s) = \frac{Cb\cos\theta}{m_2}\{H_0(s) - (1 - e^{-\tau s})X_1(s) + (1 - e^{-\tau s})X_2(s)\} \tag{13}$$

These can be simplified and a vector of transfer functions can be written of the form:

$$\frac{X(s)}{H_0(s)} = [A]^{-1}\{B\} \tag{14}$$

where

$$X(s) = \begin{Bmatrix} X_1(s) \\ X_2(s) \end{Bmatrix} \tag{15a}$$

$$[A] = \begin{bmatrix} \varphi_1 + pm_2(1 - e^{-\tau s}) & -pm_2(1 - e^{-\tau s}) \\ -pm_1(1 - e^{-\tau s}) & \varphi_2 + pm_1(1 - e^{-\tau s}) \end{bmatrix} \tag{15b}$$

$$\{B\} = \begin{Bmatrix} -pm_2 \\ pm_1 \end{Bmatrix} \tag{15c}$$

and

$$p = \frac{Cb\cos\theta}{m_1 m_2} \tag{15d}$$

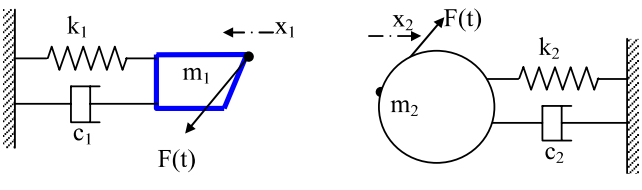

Fig. 2 Flexible workpiece model; (**a**) model of cutting tool and (**b**) model of workpiece

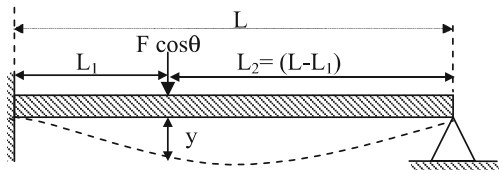

Fig. 3 Deflection of tailstock-supported workpiece

The functions $\varphi_1 = \left(s^2 + 2\xi_1\omega_{n1} + \omega_{n1}^2\right)$ and $\varphi_2 = \left(s^2 + 2\xi_2\omega_{n2} + \omega_{n2}^2\right)$ are defined for convenience.

3 Stability analysis

The stability can be analyzed by considering the characteristic equation of the system and studying the relationship between the spindle speed N and chip width b.

3.1 Rigid workpiece

For this case, Eq. 5 defines the characteristic equation as:

$$1 + bC\frac{(1 - e^{-\tau s})\cos\theta}{m_1 s^2 + c_1 s + k_1} = 0 \tag{16}$$

Substituting $s=j\omega$, separating real and imaginary terms, and solving for τ and b yields the following critical values [12]:

$$\tau^* = \frac{2}{\omega}\left\{(n + 1/2)\pi + a\tan\left[\frac{c_1\omega}{m_1\omega^2 - k_1}\right]\right\}, \tag{17a}$$

where $n = 0, 1, 2\ldots.$

$$b^* = -\frac{c_1\omega}{C\cos\theta\sin\omega\tau^*} \tag{17b}$$

Here, ω is the chatter frequency. Spindle speed in revolution per second is computed as $N=1/\tau^*$. It can be seen that Eq. 17a has multiple solutions due to different values of n. Thus, Eqs. 17a and 17b define the stability limits of this system.

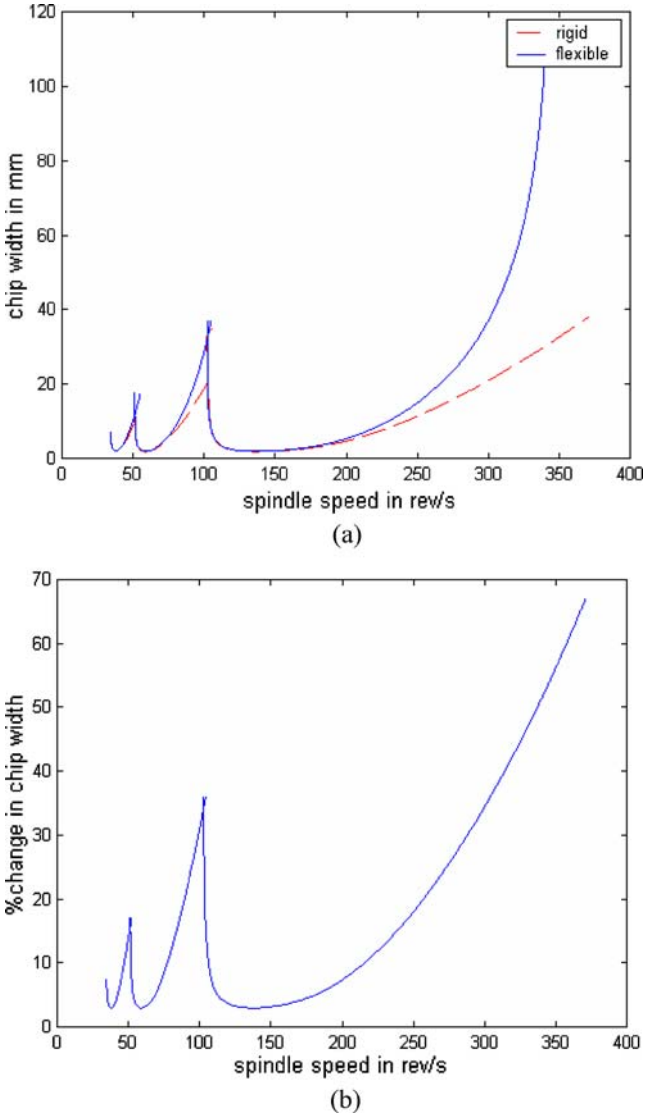

Fig. 4 **a** Comparison of lobe diagram for rigid and flexible workpiece (r=0.03 m, L=0.3 m, and L_1=0.6 L). **b** Variation of percentage difference in chip width between rigid and flexible workpiece

3.2 Flexible workpiece

As shown in Fig. 3, when the cutting is performed at any location L_1 on a tailstock-supported workpiece, the cutting force causes the workpiece to deflect. This deflection is

Table 1 Cutting tool and workpiece data [13]

Component/parameter	m (kg)	c (kg/s)	k (N/m)	C (N/m^2)	θ	E (GPa)	ρ (kg/m^3)	L (m)	r (m)
Tool	50	2×10^3	2×10^7	2×10^9	70°	–	–	–	–
Workpiece (steel)	–	–	–	–	–	180	7,850	0.5, 0.25	0.025
									0.03
									0.035
									0.04
									0.05

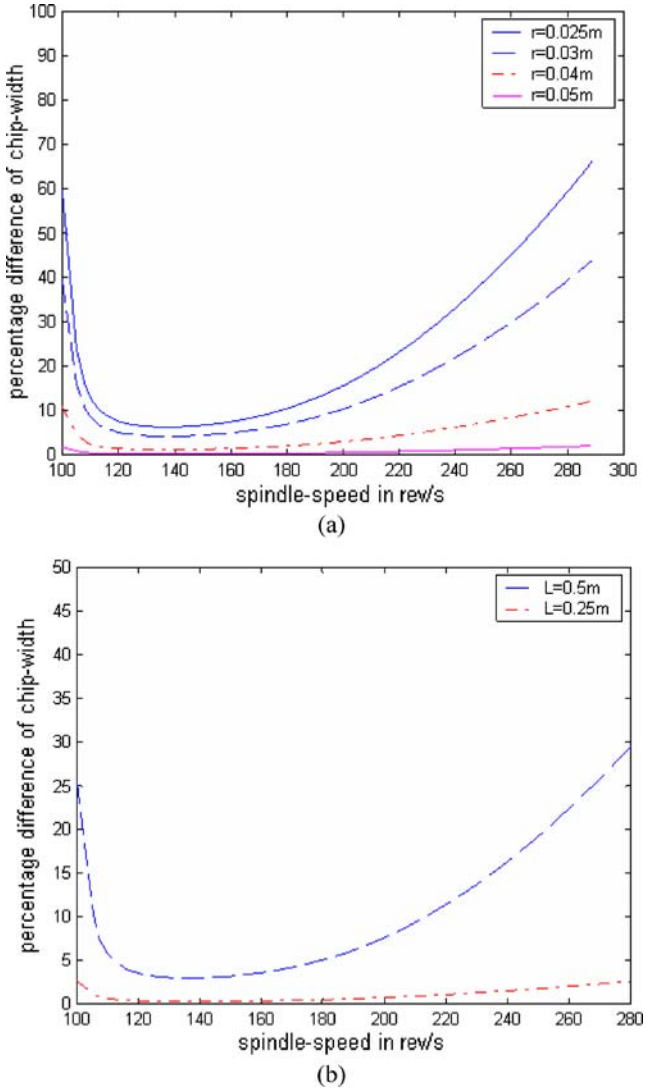

Fig. 5 **a** Variation of percentage difference in chip width with spindle speed for steel workpieces of constant length but different radii (L= 0.5 m and L_1=0.6 L, n=0). **b** Variation of percentage difference in chip width with spindle speed for steel workpieces of constant radius but different lengths (r=0.03 m and L_1=0.6 L, n=0)

accounted as stiffness of workpiece in the proposed model. Using the stiffness expression for propped cantilever model of workpiece

$$k_2 = \frac{-12L^3EI}{L_1^2L_2\{3L(L_2^2-L^2)+L_1(3L^2-L_2^2)\}} \tag{18}$$

the fundamental natural frequency of workpiece $\omega_{n2} = \sqrt{\frac{k_2}{\rho AL}}$ is obtained. Here, E is elastic modulus; ρ is material density; L is total length between the supports and I, A are respectively the cross-sectional moment of inertia and area of workpiece.

From Eqs. 14, 15a, 15b, 15c, and 15d, the characteristic equation for flexible model can be expressed as:

$$\det(A) = \begin{vmatrix} \varphi_1 + pm_2(1-e^{-\tau s}) & -pm_2(1-e^{-\tau s}) \\ -pm_1(1-e^{-\tau s}) & \varphi_2 + pm_1(1-e^{-\tau s}) \end{vmatrix}$$
$$= 0(or)\varphi_1\varphi_2 + p(1-e^{-\tau s})(\varphi_1 m_1 + \varphi_2 m_2) = 0 \tag{19}$$

Substituting $s=j\omega$ and expanding Eq. 19 and separating real and imaginary terms, it results in:

$$(a_1a_2 - b_1b_2) + p\{(1-\cos\omega\tau)A - B\sin\omega\tau\} = 0 \tag{20}$$

$$(a_1b_2 + a_2b_1) + p\{(1-\cos\omega\tau)B + A\sin\omega\tau\} = 0 \tag{21}$$

where $a_1 = (\omega_{n1}^2 - \omega^2)$, $b_1 = 2\xi_1\omega_{n1}\omega$, $a_2 = (\omega_{n2}^2 - \omega^2)$, $b_2 = 2\xi_2\omega_{n2}\omega$, $A = (m_1a_1 + m_2a_2)$, and $B = (m_1b_1 + m_2b_2)$.

Eliminating p from Eqs. 20 and 21 and defining $D = (a_1a_2 - b_1b_2)$ and $E = (a_1b_2 + a_2b_1)$, the phase shift can be written as:

$$\tan\psi = -\frac{\sin\omega\tau}{1-\cos\omega\tau} = -1/\tan\frac{\omega\tau}{2} \tag{22}$$
$$= \tan\left(\frac{\omega\tau}{2} - \frac{\pi}{2} - n\pi\right) = \frac{BD-AE}{AD+BE}$$

or

$$\frac{\omega\tau^*}{2} = \left\{(n+1/2)\pi + a\tan\left[\frac{BD-AE}{AD+BE}\right]\right\}, \tag{23a}$$

where $n = 0, 1, 2, \ldots$

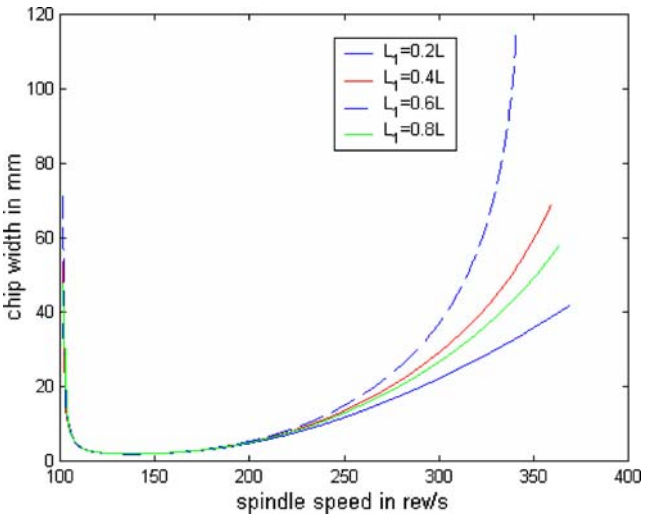

Fig. 6 Effect of position of cutting in tailstock-supported workpiece

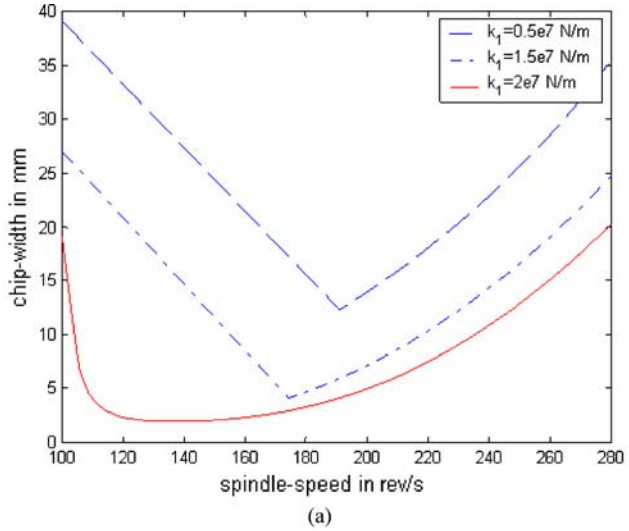

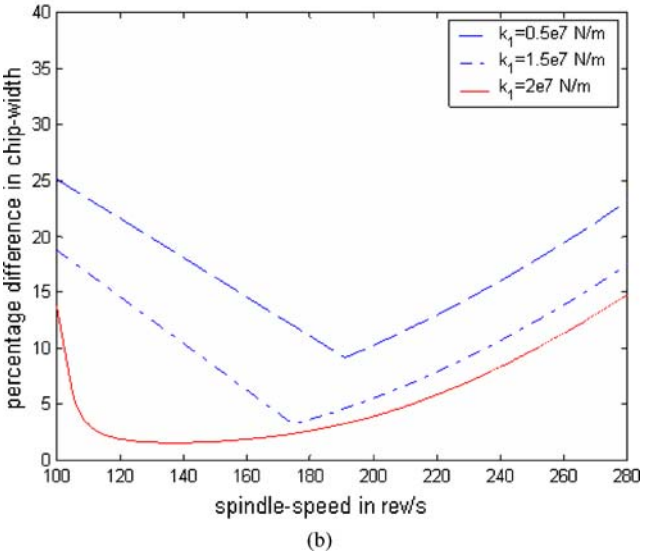

Fig. 7 **a** Variation of chip width as a function of spindle speeds at different values of cutter stiffness (L=0.5 m, r=0.35 m, n=0). **b** Variation of percentage difference in chip width with spindle speed at different values of cutting tool stiffness (L=0.5 m, r=0.35 m, n=0)

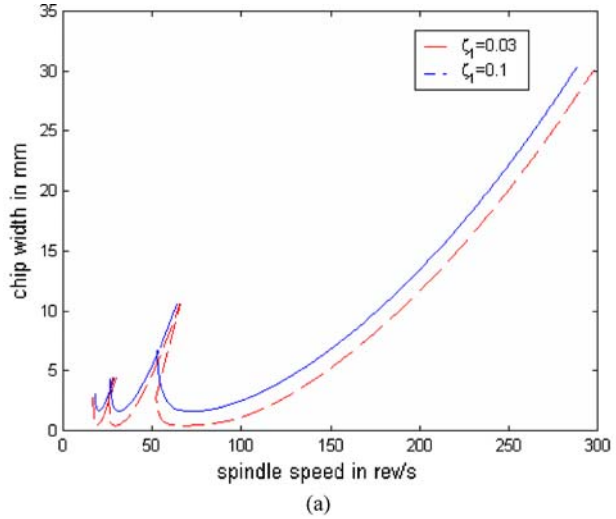

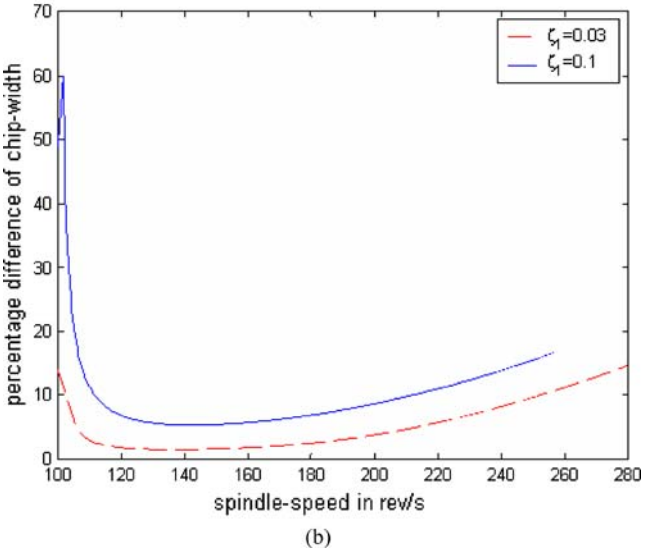

Fig. 8 **a** Variation of chip thickness with spindle speeds as a function of damping ratio of tool. **b** Variation of percentage change of chip thickness with spindle speeds as a function of damping ratio of tool (L =0.5 m, r=0.35 m, n=0, k_1=0.5×10^7 N/m)

and

$$b^* = \frac{m_1 m_2}{C\cos\theta}\left[\frac{D}{B\sin\omega\tau^* - A(1-\cos\omega\tau^*)}\right] \tag{23b}$$

These equations define stability limits for a cutting tool and workpiece. Thus, the dynamic characteristics of workpiece and cutting tool are used to obtain the stability lobe diagram.

4 Results and discussion

The stability charts are constructed from the present model in order to identify the effects of physical parameters of

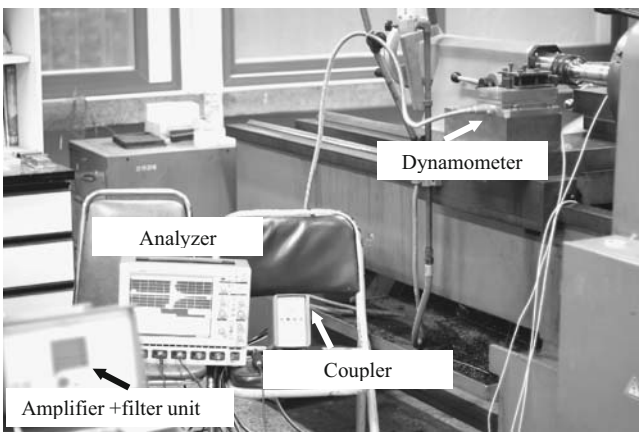

Fig. 9 Experimental setup for finding modal data

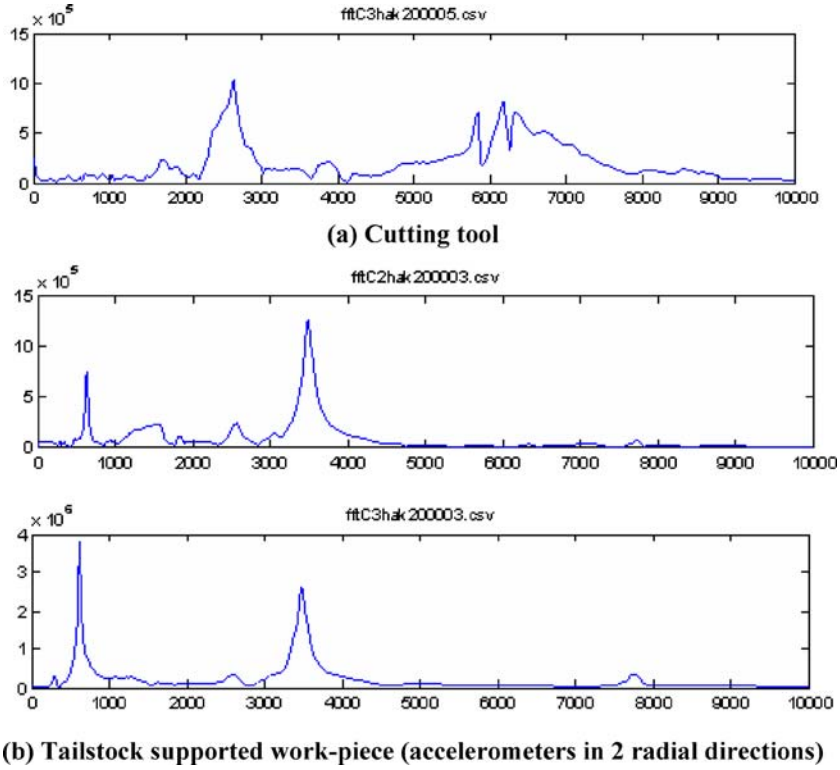

Fig. 10 **a** FFT data of acceleration response of tool. **b** FFT data of acceleration response of workpiece in two radial directions

Table 2 Major cutting conditions

Cutting tool (carbide insert)	Workpiece (AISI 1045 steel)	Cutting conditions
Natural frequency ω_{n1}= 2,500 Hz	Natural frequency ω_{n2}= 600 Hz	Cutting speeds (rpm) 740,770,800
Damping ratio ξ_1=0.015	Damping ratio ξ_2=0.023	Depth of cut (mm) 1.45–1.61
Stiffness $k_1=1.2\times10^7$ N/m	Stiffness $k_2=6.5\times10^6$ N/m	Feed (mm/rev) 0.246

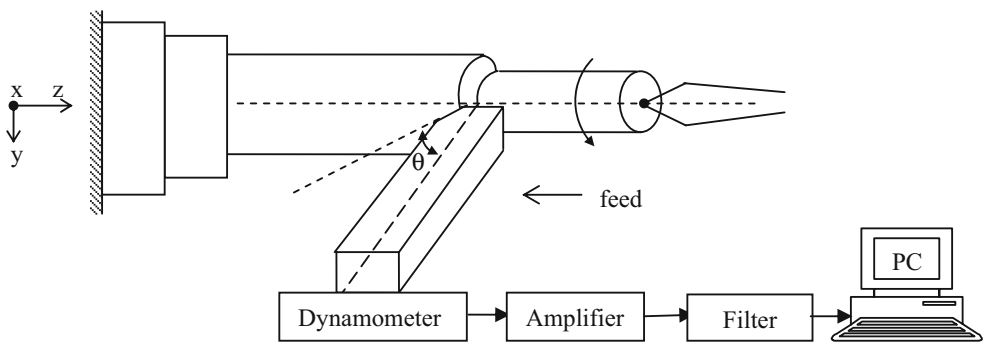

Fig. 11 Arrangement for dynamic force measurement

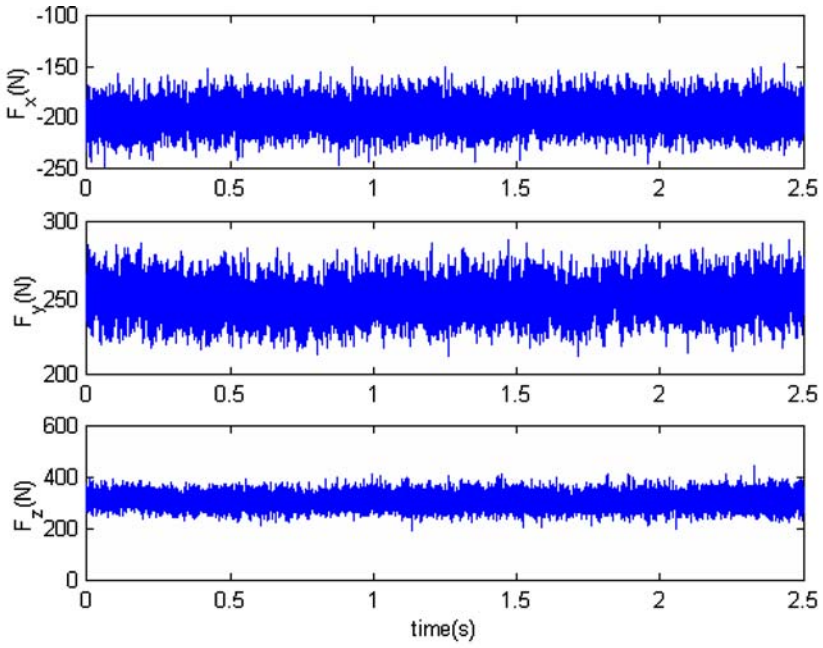

(a) Stable state (b=1.47 mm and N=770 rpm)

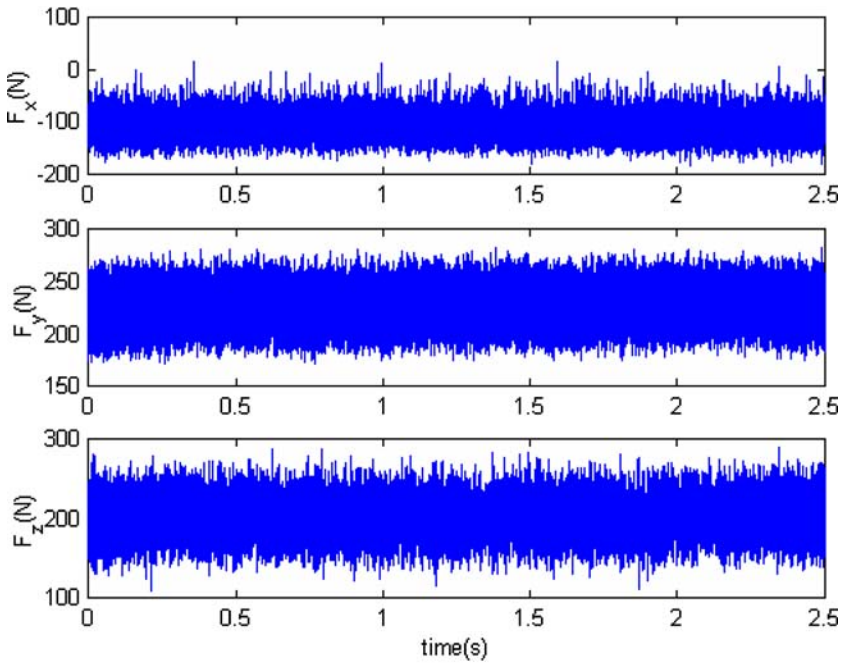

(b) Unstable state (b=1.58 mm and N=770 rpm)

Fig. 12 a, b Experimentally obtained dynamic cutting forces in two different states

workpiece and dynamic parameters of the cutting tool. In order to compare the results of the proposed model, the cutting tool and workpiece data are selected from [13] and is shown in Table 1.

4.1 Effect of workpiece dynamics

When cutting force deflects the workpiece, the effect of work deflections on stability of cutting process are shown in Fig. 4a. Here, a 0.5-m-long and 0.03-m-radius workpiece is considered. The dotted line indicates the stability curve for rigid workpiece model. It is seen that critical chip width at higher speeds is considerably large when the work flexibility is considered. Figure 4b shows the variation of percentage difference of chip width in both cases as a function of spindle speed. Large percentage differences are noticed at the right side of the diagram. This behavior is very close to available results.

Figure 5a shows variation of percentage difference in the critical chip width as a function of spindle speed for four different workpieces of constant length 0.5 m with different radii. The percentage difference has decreased progressively with increase in radius as noticed in earlier work. Figure 5b shows the variation of percentage difference in critical chip width as a function of spindle speed for two workpieces of constant radius 0.03 m, with different lengths. Larger workpiece has more deflection and has more critical chip width. In all the cases, the position of cutting tool is considered at L_1=0.6 L. The damping ratio for all workpiece conditions is taken as 0.025 since it normally varies from 0.01 to 0.05.

Figure 6 shows the influence of cutter position on chatter stability. Here, a workpiece of 0.5 m long and 0.03 m radius subjected to tool forces at points: L_1=0.2,0.4, 0.6, and 0.8 L is considered separately. As seen from the figure, critical depth of cut increases for some length (L_1=0.6 L) as the tool moves towards the tailstock and then it decreases again. Here, the cutting position (L_1) is accounted in terms of change in natural frequency of workpiece (ω_{n2}). This result is also in close agreement with results of [13].

4.2 Effect of cutting tool dynamics

Figure 7 shows the chatter stability limits, when cutting tool stiffness k_1 changes from 0.5×10^7 to 2×10^7 N/m at constant values of workpiece length L=0.5 m and radius r=0.035 m. It is seen that, as the tool becomes more flexible, critical depth of cut increases progressively. Figure 8a shows the effect of cutter damping ratio on the chatter stability for a cutter stiffness $k_1=0.5\times10^7$ N/m, along with workpiece dimensions: L=0.5 m and r=0.035 m. Figure 8b depicts the variation of percentage difference of chip width with and without considering the workpiece motion. By increasing the damping ratio of cutting tool, stability enhances only for highly flexible tools.

4.3 Experimental analysis

In order to validate the present stability lobe diagram, experiments are carried out on a 7.5-kW engine lathe with a tailstock-supported steel workpiece of 60-mm diameter and set over length 250 mm, under various operating conditions. The modal data of the workpiece and tool are obtained from standard impact hammer test. Figure 9 shows the experimental setup used for measurement of modal parameters.

An impact hammer especially designed for experimental modal analysis in laboratory (model Kistler 9724A) was used to excite the workpiece and cutting tool. To measure the vibratory response, two small piezoelectric accelerometers (model Kistler 8632C50) were used in two lateral directions. The 5134A microprocessor-controlled coupler provides power and signal processing. Figure 10 shows the transformed values of accelerometer readings in frequency domain for the cutting tool and workpiece.

For finding the experimental stability states, the major cutting conditions along with the predicted modal parameters are listed in Table 2. The cutting force coefficient (C) calculated from orthogonal data of AISI 1045 steel workpiece (using shear stress, shear angle, and friction angle with orthogonal transformations) is found to be 700 MPa. Tool with coated carbide insert employed during cutting has straight cutting edge without nose radius.

Dynamic cutting forces are recorded with a tool dynamometer in order to predict the chatter conditions. Figure 11 illustrates the arrangement for dynamic cutting force measurement.

Cutting force was measured with a Kistler 9121 three-component piezoelectric dynamometer and associated 5070 multichannel charge amplifier connected to a PC employing Kistler Dynoware force measurement software. Measurements were taken within the first 2.5 s of cut. The sampling rate used is 1 kHz.

Figure 12 shows the experimentally obtained dynamic components of three cutting forces in two different cutting states. Often, chatter generation affects mostly the cutting force in Z-direction and hence dynamic component of this force is expected to be relatively large in amplitude among the three force components. However, when chatter occurs in the radial and feed directions also, it leads to irregular distribution of chip thickness along the cutting edges. In such cases, X and Y components of force would also be large. Figure 13 shows the experimental cutting states projected over the analytical stability lobe diagram. Interestingly, the stable and unstable points are very accurately demarked by the lobe curve from the present analytical formulation.

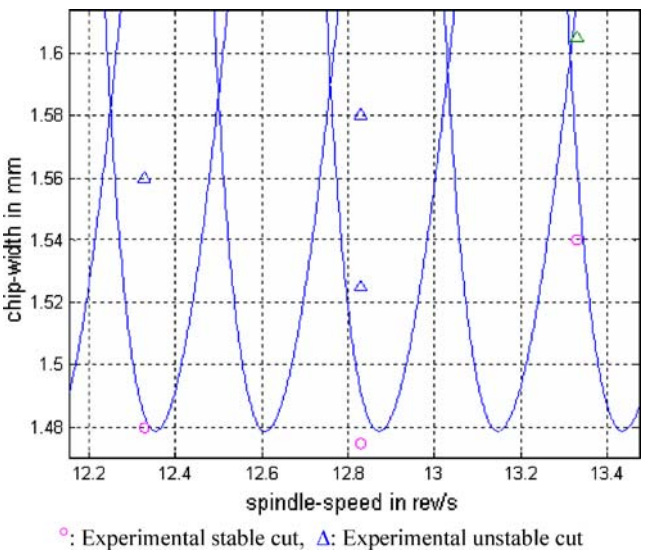

Fig. 13 Chip width predicted by present analytical model

5 Conclusions

In this paper, stability analysis in turning process has been presented with a coupled dynamic model of cutting tool and workpiece. The methodology was presented with tailstock-supported workpiece operated with a cutting tool. Effect of cutting position, workpiece dimensions, cutter flexibility, and cutter damping on the dynamic stability have been presented with the proposed dynamic model. The deviations of stable depths of cut measured by present model and existing one-dimensional rigid workpiece model have been found to be in close agreement with available works in literature. The experimental chatter predictions have revealed that the proposed model establishes the stable states accurately in rough turning operations.

References

1. Tobias SA, Fishwick W (1958) The chatter on lathe tools under orthogonal cutting conditions. Trans ASME 80:1079–1088
2. Tobias SA (1961) Machine tool vibration. Wiley, New York
3. Merrit HE (1965) Theory of self-excited machine tool chatter. J Eng Ind Trans ASME 87:447–454
4. Tlusty J (1999) Manufacturing processes and equipment. Prentice Hall, Upper Saddle River
5. Altintas Y, Weck M (2004) Chatter stability of metal cutting and grinding. Ann CIRP 53:619–642
6. Chandiramani NK, Pothala T (2006) Dynamics of 2-DOF regenerative chatter during turning. J Sound Vibrat 290:448–464 doi:10.1016/j.jsv.2005.04.012
7. Dassanayake AV, Suh CS (2008) On nonlinear cutting response and tool chatter in turning operation. Com. Nonlinear Sc. Numer. Simulations 13:979–1001 doi:10.1016/j.cnsns.2006.08.003
8. Wang ZC, Cleghorn WL (2002) Stability analysis of spinning stepped-shaft workpieces in a turning process. J Sound Vibrat 250:356–367 doi:10.1006/jsvi.2001.3725
9. Ganguli A, Deraemaeker A, Preumont A (2007) Regenerative chatter reduction by active damping control. J Sound Vibrat 300:847–862 doi:10.1016/j.jsv.2006.09.005
10. Tarng YS, Hseih YW, Li TC (1996) Automatic selection of spindle speed for suppression of regenerative chatter in turning. Int J Adv Manuf Technol 11:12–17 doi:10.1007/BF01177179
11. Carrino L, Giorleo G, Polini W, Prisco U (2002) Dimensional errors in longitudinal turning based on the unified generalized mechanics of cutting approach, part-I; 3-D theory. Int J Mach Tools Manuf 42:1509–1515 doi:10.1016/S0890-6955(02)00117-7
12. Wang M, Fei R (1999) Improvement of machining stability using a tunable-stiffness boring bar containing an electrorheological fluid. Smart Mater Struct 8:511–514 doi:10.1088/0964-1726/8/4/309
13. Chen CK, Tsao YM (2006) A stability analysis of turning tailstock supported flexible work-piece. Int J Mach Tools Manuf 46:18–25 doi:10.1016/j.ijmachtools.2005.04.002
14. Chen CK, Tsao YM (2006) A stability analysis of regenerative chatter in turning process without using tailstock. Int J Adv Manuf Technol 29:648–654 doi:10.1007/s00170-005-2573-5